Free Radical Research, April 2007; 41(4): 469–477

informa
healthcare

Methyl vinyl ketone induces apoptosis in murine GT1-7 hypothalamic neurons through glutathione depletion and the generation of reactive oxygen species

K. SATHISHKUMAR, VISWANATHAN RANGAN, XUELI GAO, & RAO M. UPPU

Department of Environmental Toxicology and the Health Research Center, Southern University and A&M College, Baton Rouge, LA 70813, USA

Accepted by Professor Dr J. Keller

(Received 17 October 2006; in revised form 22 November 2006)

Abstract

α,β-Unsaturated carbonyl compounds have been implicated in a number of environmentally-related diseases. Often, the presence of α,β-unsaturated carbonyl functionality as part of either an aliphatic or cyclic structure is considered a structural alert for cytotoxicity. We examined the cytotoxicity of methyl vinyl ketone (MVK), an aliphatic, straight-chain α,β-unsaturated carbonyl compound, in murine GT1-7 hypothalamic neurons. In addition to its widespread environmental occurrence, MVK was selected due to its extensive use in the chemical industry. Also, MVK is a close structural analog of hydroxymethylvinyl ketone that, in part, mediates the cytotoxic effects of 1,3-butadiene *in vivo*. It was found that MVK at low micromolar concentrations induced extensive cell death that retained key features of apoptosis such as chromatin condensation and DNA fragmentation. The MVK-induced apoptosis was associated with depletion of glutathione, disruption of mitochondrial transmembrane potential, and increased generation of reactive oxygen species (ROS). Supplementation of neuronal cells with Trolox offered partial, but significant, protection against the MVK-induced cytotoxicity, presumably due to scavenging of ROS *in situ*. The suggested sequence of events in the MVK-induced apoptosis in neuronal cells involves the depletion of cellular glutathione followed by an increased generation of ROS and finally the loss of mitochondrial function.

Keywords: *Apoptosis, glutathione, methyl vinyl ketone, reactive oxygen species, Trolox, α,β-unsaturated carbonyl compounds*

Introduction

α,β-Unsaturated carbonyls represent an important class of mutagenic/genotoxic compounds to which humans are routinely exposed. The sources of exposure include diet (2-hexenal), endogenous production (4-hydroxy-2-nonenal), and environment (methyl vinyl ketone or MVK). α,β-Unsaturated carbonyls present a potential health risk due to their reactivity towards cellular nucleophiles such as amines and thiols, forming 1,4- or 1,6-addition (Michael) products. MVK is considered as a prototype of the straight-chain, aliphatic α,β-unsaturated carbonyl compounds [1] with widespread scope for environmental exposure. Commercially, MVK is used in the production of pesticides [2], perfumes [3], plastics and resins [4,5], and as a pharmaceutical intermediate in the synthesis of steroids, vitamin A, and anticoagulants [6–8]. MVK is present in tobacco smoke (0.13 mg/cigarette) [9–11] and automobile exhaust [12,13]. It can be formed in the atmosphere via photochemical, presumably ozone-mediated, degradation of isoprene among many biogenic and anthropogenic hydrocarbons [14,15]. MVK is a close structural analog of hydroxymethylvinyl ketone (HMVK) that, in part,

Correspondence: Rao M. Uppu, Department of Environmental Toxicology and the Health Research Center, Southern University and A&M College, 108 Fisher Hall, James L. Hunt Street, Baton Rouge, LA 70813, USA. Tel: 1 225 771 5133. Fax: 1 225 771 5350. E-mail: rao_uppu@subr.edu

ISSN 1071-5762 print/ISSN 1029-2470 online © 2007 Informa UK Ltd.
DOI: 10.1080/10715760601145257

mediates the toxicity of 3-butene-1,2-diol via biotransformation involving CYP 2E1 and, possibly, alcohol dehydrogenase [16–20].

The cytotoxic properties of MVK received much less attention than those elicited by acrolein and crotonaldehyde (CA), the two other α,β-unsaturated carbonyl compounds commonly found in polluted air [21,22]. Acrolein and CA have been shown to be formed *in vivo* [23–25], possibly as a result of lipid peroxidation [25,26]. The available literature, although scanty, suggests that MVK is highly toxic to certain cell types such as isolated rat kidney cells [27–29] and hepatocytes [30]. Although described as a Michael acceptor capable of alkylating proteins and nucleic acids [28,31], the mechanism(s) by which MVK exerts its cytotoxic effects is not completely understood. In the present communication, we compared the cytotoxicity of acrolein, CA and MVK and examined, in detail, the mechanism(s) of MVK-induced cell death in murine GT1-7 hypothalamic neurons. We observed that MVK was more toxic than acrolein and CA. A further examination of the molecular basis of cytotoxicity revealed that MVK depletes cellular glutathione and promotes the generation of reactive oxygen species (ROS). The cell death induced by MVK has been shown to be typical of apoptosis, and it could be prevented by antioxidant supplementation.

Materials and methods

Materials

Chemicals and reagents for cell culture were obtained as follows: Acrolein (90%), CA(99%), and MVK (99%) from Aldrich (Milwaukee, WI); *N*-acetyl-L-cysteine (NAC), Dulbecco's modified eagle's medium (DMEM), Fetal bovine serum (FBS), Hank's balanced salt solution (HBSS), phosphate buffered saline (PBS), penicillin–streptomycin, and trypsin-EDTA from Sigma (St Louis, MO); Trolox from Calbiochem (San Diego, CA); and acridine orange, ethidium bromide, and 5-(and-6)-chloromethyl-2′,7′-dichlorodihydrofluorescein diacetate (CM-H_2DCFDA) from Invitrogen (Carlsbad, CA). Cell culture flasks and 24-well culture plates were purchased from Corning (Acton, MA). Kits for non-radioactive cell proliferation assay, nucleosomal DNA fragmentation, mitochondrial membrane potential and glutathione enzymatic recycling assay were obtained from Promega (Madison, WI), Roche (Indianapolis, IN), Calbiochem (Sandiego, CA) and Biovision (Mountain View, CA), respectively. All other chemicals and reagents were of the highest grade available.

Immortalized murine GT1–7 hypothalamic neurons [32] were a generous gift from Dr Pam Mellon (University of California; San Diego, CA). Unless mentioned otherwise, the neuronal cells were grown in T25/T75 flaks in DMEM supplemented with 10% FBS and antibiotics (penicillin, 10 units/ml and streptomycin, 100 μg/ml) in 5% CO_2/95% air saturated with humidity at 37°C [33,34].

Stock solutions of acrolein, CA, and MVK were prepared in PBS (50 mM; pH 7.4) just before use. Trolox was dissolved in ethanol at a concentration of 0.25 M, and NAC in PBS at a concentration of 0.5 M (pH adjusted to 7.4). The solutions of Trolox and NAC were stored at −20°C until use.

Exposure of neuronal cells to acrolein, CA, and MVK

All experiments were performed using murine GT1-7 hypothalamic neurons grown to sub-confluency in 24-well plates. Just before exposure to MVK, the neuronal cells were washed once with PBS. Exposure to MVK (1–30 μM) was performed typically for 2 h at 37°C in HBSS that did not contain FBS. At the end of the exposure period, neuronal cells were washed free of MVK (using PBS) and a fresh medium of DMEM, supplemented with 10% FBS, but devoid of MVK, was added. Neuronal cells, with or without prior exposure to MVK, were cultured for an additional 24 h and then assayed for viability, DNA fragmentation, glutathione, ROS, and mitochondrial transmembrane potential. It was found that serum deprivation for 2 h did not result in any significant loss of neuronal cell viability. Similar protocols were followed for exposure of neuronal cells to acrolein (10–500 μM) and CA (10–500 μM).

Antioxidant supplementation

Stock solutions of Trolox and NAC were diluted with HBSS to the required working concentration(s). Neuronal cells were pre-incubated with Trolox (500 μM) or NAC (5 mM) for 1 h and then exposed to MVK (1–30 μM) for 2 h in HBSS containing antioxidants. At the end of the incubation period, cells were washed and a fresh medium of DMEM containing 10% FBS and antioxidants (500 μM Trolox or 5 mM NAC) was added. The cells were assayed for viability, DNA fragmentation, glutathione and ROS after 24 h as described above. Control experiments were performed by adding appropriate amounts of either ethanol or PBS.

Analysis of cell viability

The viability of hypothalamic neurons was assessed as described earlier [35,36] based on the reduction of 3-(4,5-dimethylthiazol-2-yl)-5-(3-carboxymethoxyphenyl) 2-(4-sulfophenyl)-2H-tetrazolium (MTS) to a water-soluble formazan by NADH, NADPH and, possibly, $FADH_2$ [37,38] present in metabolically active cells. The transfer of reducing equivalents was facilitated through use of phenazine methosulfate (PMS) supplied as part of CellTiter96 Aqueous One cell proliferation assay kit.

Dual staining of neuronal cells using acridine orange and ethidium bromide

A cell-permeable dye, acridine orange (AO) emits green fluorescence upon intercalation into double-strand DNA allowing visualization of the nuclear chromatin pattern [39]. Ethidium bromide (EB) stains DNA orange, but is excluded by viable cells [40]. We used this dual staining to visualize: (i) living cells (uniformly stained green nucleus); (ii) cells in early apoptosis (cell membrane is continuous but chromatin is condensed with an irregular green nucleus) [2]; (iii) cells in late apoptosis (orange nuclei with condensed or fragmented chromatin; this stage is also referred to as secondary necrosis or apoptotic necrosis); and (iv) necrosis (uniform orange-colored nuclei). Immediately following addition of AO/EB (100 μg/ml each), the neuronal cells were examined for the four stages mentioned above in three independent experiments. Images were captured using a Nikon Optiphot microscope equipped with CoolSNAP camera (Photometrics; Tucson, AZ). Image capture and analysis were performed using MetaMorph software (Molecular Devices; Sunnyvale, CA). The results are expressed as a percentage of apoptotic (stages ii and iii) and/or necrotic cells (stage iv) produced in response to treatment with MVK in the presence and absence of added antioxidants.

Quantitation of DNA fragmentation by ELISA

Apoptosis is characterized by nucleosomal DNA fragmentation. We measured DNA fragmentation using a specific two-site ELISA kit from Roche (Indianapolis, IN) based on the application of an anti-histone primary antibody and a secondary anti-DNA antibody conjugated to horseradish peroxidase. The assay was performed as follows. Neuronal cells were lysed in 200 μl of buffer provided by the manufacturer, the nuclei and cell debris were removed by centrifugation (200*g*; 10 min), and the supernatants (cytosol containing low-molecular mass, fragmented DNA) were diluted 3-fold with the buffer used for cell lysis. Aliquots (20 μl each) of the diluted cytosolic fractions were transferred to a 96-well plate that was pre-coated with anti-histone antibody and an immunoreagent mix (80 μl each) containing a secondary anti-DNA antibody-peroxidase conjugate was added to each well. After incubation and required washing procedures, the activity of peroxidase associated with the anti-DNA antibody bound to the microtiter plate was measured based on oxidation of 2,2′-azinobis(3-ethylbinzthiazoline) sulfonic acid (ABTS) to $ABTS^{\cdot+}$. A BioTek EL 800 microplate reader was used to measure $ABTS^{\cdot+}$ at 405 nm. The results are expressed as folds-increase relative to the untreated controls.

Estimation of oxidized and reduced glutathione

Total glutathione (GSH + GSSG) in hypothalamic neurons was measured using an enzyme recycling assay kit (Biovision; Moutain view, CA). Briefly, after washing with PBS, neuronal cells were lysed in 300 μl of ice-cold buffer supplied by the manufacturer, the lysate was centrifuged at 10,000*g* for 15 min at 4°C, and the supernatant was separated. A microplate, high throughput assay was performed on the supernatant (20 μl) by adding glutathione reductase, reagents for NADPH regeneration, and 5,5′-dithiobis-(2-nitrobenzoic acid) to the sample (final volume: 200 μl). After 10 min of incubation at room temperature, 5-thio-2-nitrobenzoate formed was measured at 405 nm using a BioTek EL 800 microplate reader. The concentration of total glutathione was calculated from a standard curve after normalization for cell numbers. To measure GSSG alone, GSH in the supernatants was derivatized by incubation with 2-vinylpyridine (final concentration: 10 mM) for 1 h at room temperature, and the assay of glutathione was then performed as described above. The results are expressed as a percentage decrease in glutathione content compared to the untreated controls.

Measurement of intracellular ROS

Neuronal cells were loaded by incubation with 10 μM CM-H_2DCFDA in Krebs-Ringer/HEPES (KRH) buffer (115 mM NaCl, 5 mM KCl, 1 mM KH_2PO_4, 1.5 mM $CaCl_2$, 1.2 mM $MgSO_4$, 5 mM glucose, and 25 mM HEPES, pH 7.4) for 30 min at 37°C. After loading, the cells were washed twice with fresh KRH buffer and kept at room temperature for 20 min. The cells were exposed to different concentrations of MVK and the changes in fluorescence were measured for 8 h using a microplate reader (Spectramax EM Gemini; Molecular Devices, Sunnyvale, CA) at excitation and emission wavelengths of 480 and 530 nm, respectively. The fluorescence generated by control cells was subtracted from the treated samples and expressed as percent increase in raw fluorescence units over the controls.

Measurement of mitochondrial transmembrane potential

The mitochondrial transmembrane potential ($\Delta\Psi_m$) in neuronal cells treated with 1, 5 and 10 μM MVK for 2 h was monitored using a MitoCapture kit (Calbiochem, San Diego, CA). The assay is based on accumulation of a cationic dye, 5,5′,6,6′-tetrachloro-1,1′,3,3′-tetraethylbenzimi-dazolylcarbocyanine iodide (JC-1), in mitochondria which is dependent on transmembrane potential ($\Delta\Psi_m$). The dye remains in monomeric form and exhibits green fluorescence when the value of $\Delta\Psi_m$ is small. On the other hand, at high $\Delta\Psi_m$, there is greater accumulation of the dye forming J-aggregates,

and the fluorescence shifts to red (E_{max} 590 nm). After 24 h of MVK treatment, JC-1 was added to the neuronal cells and incubated for 30 min at 37°C. The unbound dye was removed by washing with PBS and a fresh medium (500 μl; provided as part of the kit) was added, and the fluorescence was quantified at excitation and emission wavelengths of 488 and 590 nm, respectively. A Spectramax EM Gemini spectrofluorimeter was used to measure the fluorescence. The results are expressed as a percentage decrease in $\Delta\Psi_m$ compared to the untreated controls.

Statistical analysis and data presentation

Values of LC_{50} were calculated by fitting the log concentration-response curves by standard non-linear regression analysis using GraphPad Prism 4.0 Software (San Diego, CA). Data are presented as mean ± SEM of at least three separate experiments or as indicated. Statistical analyses were performed using a one-way analysis of variance (ANOVA) and Bonferroni's method for multiple comparisons. Probability of $p < 0.05$ was considered statistically significant.

Results

Cytotoxicity of acrolein, CA, and MVK in neuronal cells

Figure 1 shows the data on viability/proliferation of murine GT1-7 hypothalamic neurons exposed to the three most commonly occurring α,β-unsaturated compounds in the environment and *in vivo*. The concentration of MVK at the half-maximal lethality (LC_{50}) was 9 ± 4.1 μM. This value was 3–4-times lower than that observed with acrolein (30 ± 3.7 μM) and CA (47 ± 8.1 μM), meaning that MVK is the most potent carbonyl compound in inducing cytotoxicity in neuronal cells under the present experimental conditions.

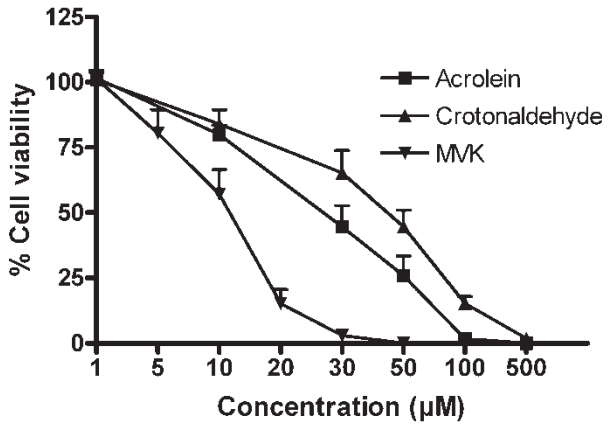

Figure 1. Cytotoxicity of acrolein, CA, and MVK in murine GT1-7 hypothalamic neurons. Neuronal cells were incubated with various low concentrations of acrolein, CA, and MVK for 2 h at 37°C. After 24 h of incubation, the viability/proliferation of MVK-exposed neuronal cells was measured based on the MTS reduction assay. Data represent mean ± SEM of 3–5 independent experiments.

MVK induces apoptosis in murine GT1-7 hypothalamic neurons

Apoptosis is characterized by a variety of morphological features. Change(s) in the nuclear morphology is one of the earliest events that could be detected easily. We observed that MVK exposure resulted in chromatin condensation and fragmentation (Figure 2(A)). The normal morphology of neuronal cells, as seen under the fluorescent microscope, consisted of green nuclei with intact structure. When treated with MVK, the cells exhibited membrane blebbing, chromatin condensation, and formation of apoptotic bodies (Figure 2(A), (a)–(d)). The changes were concentration- and time-dependent (Figure 2(B),(C)). Supplementation with Trolox at a final concentration of 200 and 500 μM reversed the MVK-induced apoptosis by 36 and 82%, respectively (Figure 2(D)).

The apoptotic response of neuronal cells to MVK exposure was confirmed by DNA fragmentation measured by ELISA. There was a dose-dependent (Figure 3(A)) and time-dependent (Figure 3(B)) increase in the occurrence of histone-associated DNA fragments. Pretreatment with Trolox (500 μM) offered substantial protection (84 ± 7.9%) against the MVK-induced DNA fragmentation. Trolox, by itself, did not have any effect on DNA fragmentation in neuronal cells.

Effect of MVK on intracellular glutathione and modulation by Trolox and NAC

We reasoned that MVK, being a potent electrophile, would cause depletion of intracellular GSH. To examine this possibility, we studied the levels of glutathione, oxidized (GSSG) as well as reduced (GSH), in MVK-exposed neuronal cells. As shown in Figure 4, MVK treatment caused a dose-dependent decrease in total glutathione. The oxidized glutathione was undetectable in both control and neuronal cells treated with MVK. This shows that glutathione depletion in MVK treatments was mainly due to a decrease in GSH, a process that was not coupled with increased GSSG. Supplementation with Trolox (500 μM) restored, in part, the MVK-induced depletion of glutathione (Figure 4). We observed a near total restoration of glutathione levels in the MVK-treated neuronal cells by supplementation with NAC (5 mM) (data not shown). The effect of NAC was most likely due to a direct scavenging of MVK, making it either ineffective or not available to neuronal cells. Control cells treated with Trolox alone did not result in significant changes in cellular glutathione levels.

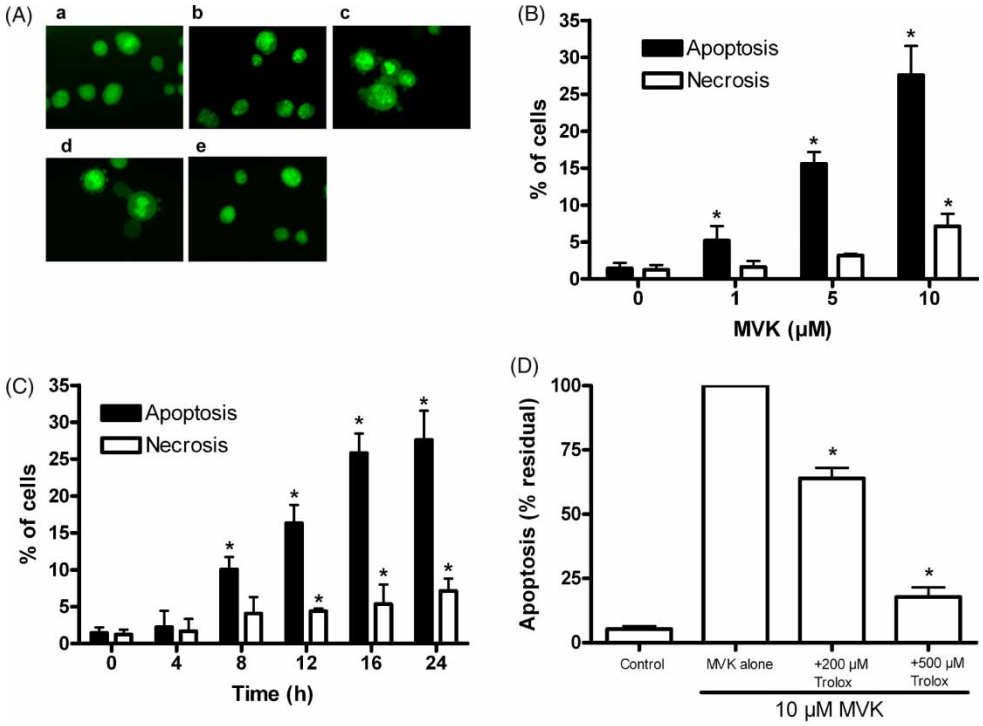

Figure 2. Dual (AO/EB) staining of murine GT1-7 hypothalamic neurons exposed to MVK. (A) Neuronal cultures exposed to MVK (1–10 μM) for 2 h were examined after 24 h for the presence of apoptotic and necrotic cells: (a) none; (b) 1 μM MVK; (c) 5 μM MVK; (d) 10 μM MVK; and (e) 10 μM MVK plus 500 μM Trolox. The cells were stained with AO/EB (100 μg/ml each) and their morphologies observed immediately under a fluorescent microscope (magnification: × 400). Cells with membrane blebbing and chromatin condensation as dense orange areas represent apoptotic cells. (B) Dose-response of MVK-induced apoptosis and necrosis measured by AO/EB dual staining. * Indicates $p < 0.05$ vs. corresponding untreated neuronal cells. (C) Time-dependent increase in apoptosis induced by 10 μM MVK. * Indicates $p < 0.05$ vs. corresponding untreated neuronal cells. (D) Protective effects of Trolox (200–500 μM) against the MVK (10 μM)-induced apoptosis in neuronal cells. Cells that contained Trolox alone (not treated with MVK), did not have any changes in cellular morphologies. * Indicates $p < 0.05$ vs. MVK (10 μM)-treated neuronal cells. Data are mean ± SEM of three independent experiments.

MVK-induced generation of ROS and its scavenging by Trolox

We examined ROS production in murine GT1-7 hypothalamic neurons exposed to MVK. Neuronal cells showed a marked increase in ROS production when exposed to MVK, and the response was found to be dose-dependent (Figure 5(A)). An increase in ROS production up to 5-fold could be seen as early as 1 h following the exposure to MVK as compared to control cells at the corresponding time point (Figure 5(B)). The MVK-induced ROS production continued for up to 8 h and tended to plateau thereafter (Figure 5(B)). Incubation of MVK-exposed neuronal cells with Trolox (500 μM) resulted in a

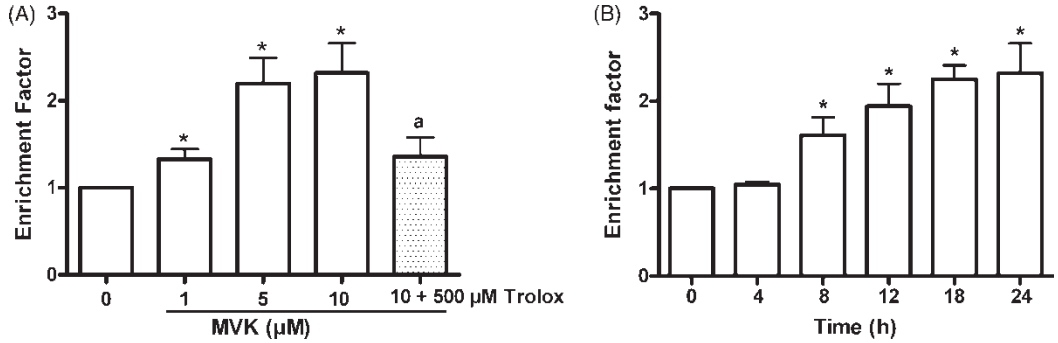

Figure 3. DNA fragmentation measured by ELISA and effect of Trolox supplementation in murine GT1-7 hypothalamic neurons exposed to MVK. (A) Dose-dependent increase in DNA fragmentation in neurons exposed to MVK and the protective effect of Trolox. (B) Time-dependent increase in DNA fragmentation in neurons exposed to 10 μM MVK. Neuronal cells were exposed to MVK (1–10 μM) for 2 h in the presence and absence of Trolox (500 μM). After indicated time points, DNA fragmentation was measured by ELISA. Values presented represent folds increase in DNA fragmentation relative to the untreated controls. Data are mean ± SEM of 3–5 independent experiments. *Indicates $p < 0.05$ vs. untreated cells; and $^{a}p < 0.05$ vs. neuronal cells treated with 10 μM MVK.

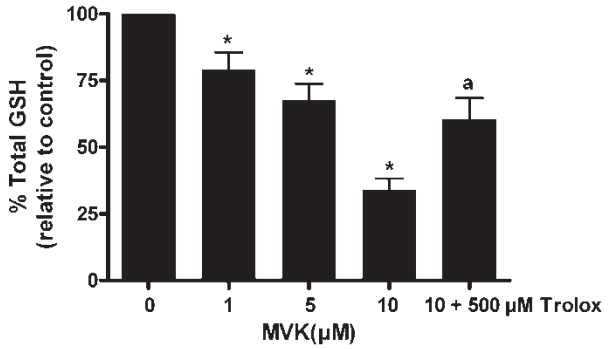

Figure 4. Levels of glutathione in murine GT1-7 hypothalamic neurons exposed to MVK and the effect of Trolox. Neuronal cells, with or without Trolox (500 µM) supplementation, were exposed to 1–10 µM MVK for 2 h. After 24 h, glutathione (GGSG and GSH) was estimated based on an enzymatic recycling assay. The values were normalized for cell numbers and expressed relative to the untreated group(s). The results are mean ± SEM of three independent experiments. ⋆ Indicates $p < 0.05$ vs. untreated cells; and $^{a}p < 0.05$ vs. neuronal cells treated with 10 µM MVK.

substantial decrease in the yields of ROS (Figure 5(B)). The effect of Trolox was most likely due to direct scavenging of ROS, making it less available for reaction with the probe CM-H_2DCF. Trolox, by itself, did not bring about any significant changes on ROS production in neuronal cells not exposed to MVK.

MVK treatment causes disruption of mitochondrial transmembrane potential

We measured mitochondrial transmembrane potential ($\Delta\Psi_m$) as its disruption reflects one of the earliest events in apoptosis. The cationic dye JC-1 accumulates in the mitochondria of normal cells giving a maximal fluorescence at 590 nm (100%). In cells undergoing apoptosis, the dye accumulation in the mitochondria is expected to be lower, provided there is a decrease in transmembrane potential. As shown in Figure 6(A), we do find evidence for lowering of $\Delta\Psi_m$ in neuronal cells exposed to MVK. The response was found to be dose-dependent with decreases in $\Delta\Psi_m$ of 18, 28 and 67% at MVK concentrations of 1, 5 and 10 µM, respectively. The decrease in $\Delta\Psi_m$ induced by 10 µM MVK was time-dependent with maximum effect being observed at 16–24 h after exposure to MVK (Figure 6(B)).

MVK-induced cytotoxicity is prevented by antioxidants

The dose–response curve for MVK-induced cytotoxicity in neuronal cells shifted to the right in the presence of Trolox (500 µM) (Figure 7). The value of LC_{50} was substantially higher (20 ± 2.5 µM), compared to the cells that were not treated with Trolox (LC_{50} 9 ± 4.1 µM; see Figure 1). Pretreatment of neuronal cells with NAC (5 mM) completely protected against MVK-induced cytotoxicity over 1–30 µM concentrations of MVK (Figure 7). Both NAC and Trolox by themselves were without any effect on neuronal cell viability.

Discussion

The results of the present study demonstrate that acrolein, CA, and MVK are highly cytotoxic to murine GT1-7 hypothalamic neurons. The cytotoxicity of MVK, which was studied in detail, conforms to an apoptotic process based on nuclear morphology and DNA fragmentation. The apoptotic response appears to be due to mitochondrial dysfunction and enhanced cellular oxidative stress status. Antioxidants such as Trolox attenuated, in part, the cytotoxic affects of MVK.

Methyl vinyl ketone appears to be somewhat more cytotoxic than acrolein and CA. Although the reasons

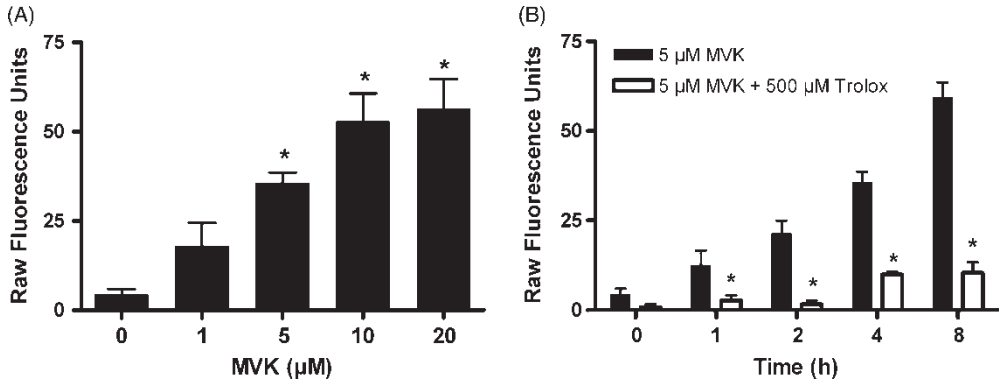

Figure 5. Generation of intracellular ROS in neuronal cells exposed to MVK and the effect of supplementation with Trolox. (A) Dose-dependent increase in ROS measured after 4 h of MVK exposure. Neuronal cells were exposed to 1–20 µM MVK for 2 h and the generation of ROS was measured by uptake, hydrolysis and subsequent oxidation of CM-H_2DCFDA. ⋆ Indicates significance $p < 0.05$ vs. untreated cells. (B) Time course of DCF generation by GT1-7 cells exposed to 5 µM MVK in the presence and absence of antioxidant (500 µM Trolox). Data are mean ± SEM of three independent determinations. ⋆Indicates $p < 0.05$ vs. untreated cells; and $^{a}p < 0.05$ vs. neuronal cells treated with 5 µM MVK at the corresponding time point(s).

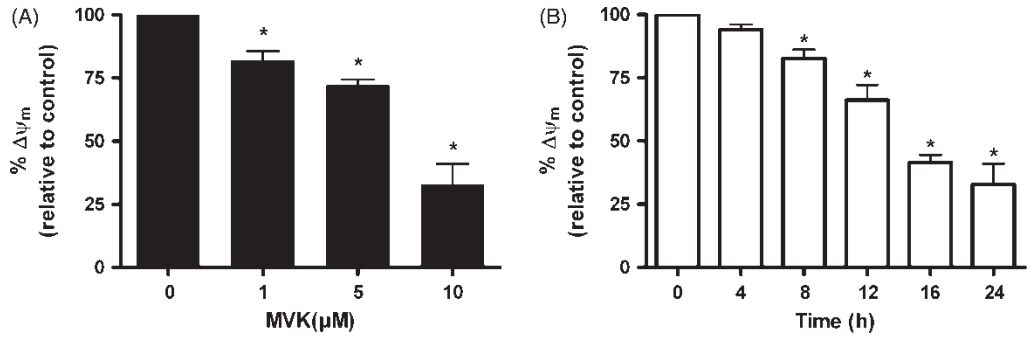

Figure 6. Changes in mitochondrial membrane potential in murine GT1-7 hypothalamic neurons exposed to MVK. (A) Dose-dependent decrease in mitochondrial membrane potential in neurons exposed to 1–10 μM MVK. (B) Time-dependent decrease in mitochondrial membrane potential in neurons exposed to 10 μM MVK. Neuronal cells were exposed to MVK for 2 h. After indicated time points, the transmembrane potential were measured using the MitoCapture apoptosis detection kit as described in the Methods section. *Indicates $p < 0.05$ vs. untreated controls.

for this are not clear at present, the results are consistent with an observation of relatively higher toxicity of MVK reported in renal tubular cells [28]. The formation of higher amounts of linear, but not cyclic, adducts by MVK than acrolein can offer an explanation [30]. Among other factors that could contribute to the observed differences in cytotoxicity is that MVK has a greater reactivity towards cellular nucleophiles such as GSH and protein thiols [41]. The lower toxicity of acrolein and, possibly CA, may also be due to differences in their detoxication by glutathione-S-transferase [42] and aldehyde dehydrogenase [43]. It is pertinent to mention here that, in rat hepatocytes, acrolein and MVK have comparable cytotoxicity [30]. However, such an outcome could be due to a multitude of defence mechanisms operating in hepatocytes.

Although there have been some reports of MVK-induced cell death in renal tubular cells [28] and hepatocytes [30], the present study reports for the first time that the neuronal cell death induced by MVK is typical of apoptosis. The disruption of mitochondrial $\Delta\Psi_m$ (Figure 6) indicates the involvement of the mitochondrial pathway in neuronal cell apoptosis. However there could be other pathways involved in MVK-induced apoptosis, and this needs to be examined further.

The lowered levels of glutathione (Figure 4) and higher production of ROS (Figure 5) in neuronal cells exposed to MVK suggest that oxidative stress status is an important determinant in the mediation of cytotoxicity. This conclusion derives further support from the observation that Trolox offers significant protection against cytotoxicity (Figure 7) by scavenging ROS (Figure 5). *N*-Acetyl-L-cysteine offered a better protection than Trolox in all these assays. We could not pledge the significance of these findings for reasons that NAC forms 1,4-addition (Michael) products with MVK, making the latter unavailable to neuronal cells.

A number of studies have shown that glutathione depletion alone can cause apoptosis in a variety of cell types [44–46]. In general, in cells undergoing apoptosis, glutathione synthesis is blocked at certain point of time [47]. In all our assays, the neuronal cells were exposed to MVK for only 2 h and the MVK-exposed cells do not recoup glutathione 24 h later. This shows that a similar mechanism of blockage of glutathione synthesis might be operating in neuronal cells. A slightly higher level of glutathione in neuronal cells supplemented with Trolox (Figure 4) could be due to a sparing effect on newly synthesized GSH.

It is important to mention that supplementation with antioxidants after MVK exposure did not sufficiently protect the neuronal cells. This may be because the 2 h exposure was sufficient to initiate the signaling events that culminate in cell death. Similarly, attempts to load the cells with antioxidants prior to MVK treatment also failed to inhibit the cytotoxicity. It was necessary that antioxidants be present during

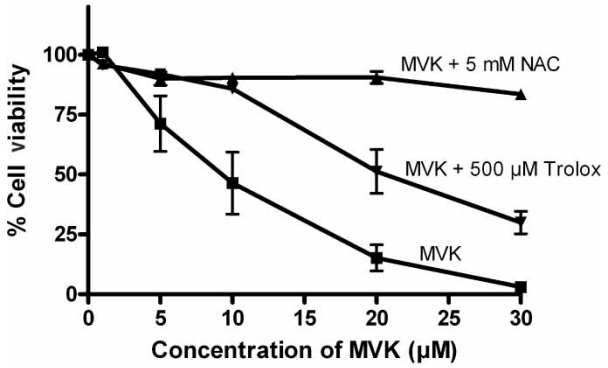

Figure 7. Protective effects of NAC and Trolox on MVK-induced cytotoxicity in murine GT1-7 hypothalamic neurons. Neuronal cells were exposed to 1–30 μM MVK in the presence and absence of NAC (5 mM) and Trolox (500 μM). After 24 h, the viability/proliferation of neuronal cells was measured by the MTS reduction assay. Data represent the mean ± SEM for three independent experiments.

and after MVK exposure to offer significant cytoprotection. The complete protection offered by NAC might be an artifact (discussed above), and for this reason, we used only Trolox to exemplify the anti-apoptotic effects of antioxidants.

General implications

There have been many reports concerning the formation of α,β-unsaturated carbonyl compounds as products of lipid peroxidation and mediation of oxidative damage in a variety of neuronal diseases (see review [48]). A large pool of antioxidants in the brain helps to combat the cytotoxic effects of these carbonyl compounds. But the antioxidant pools are decreased in several disease-related conditions [49–54]. The cytotoxic effects of MVK reported here are thought to be useful in understanding the factors that contribute to the toxicity of short-chain unsaturated carbonyls in neuronal cells. The suggested sequence of events in MVK-induced apoptosis in murine GT1-7 hypothalamic neurons involves the depletion of cellular glutathione followed by increased generation of ROS and finally the loss of mitochondrial function.

Acknowledgements

We thank Dr Pam Mellon for providing murine GT1-7 hypothalamic neurons and Dr Deidra Atkins-Ball for critical reading of the manuscript. This publication was made possible by National Institutes of Health (NIH) Grants ES 10018 (from the ARCH Program of the National Institute of Environmental Health Sciences) and P20 RR16456 (from the BRIN Program of the National Center for Research Resources), and National Science Foundation (NSF) Grant HRD 0450375 to RU. Its contents are solely the responsibility of the authors and do not necessarily represent the official views of the NIH or NSF.

References

[1] Morgan DL, Price HC, O'Connor RW, Seely JC, Ward SM, Wilson RE, Cunningham MC. Upper respiratory tract toxicity of inhaled methylvinyl ketone in F344 rats and B6C3F1 mice. Toxicol Sci 2000;58:182–194.

[2] Chuman T, Guss PL, Doolittle RE, McLaughlin JR, Tumlenson JH III. 6,12-dimethylpentadecan-2-one and its use in monitoring and controlling the banded cucumber beetle. Patent US 4,871,537; 1989.

[3] Giersch W, Schulte-Elte KH. Preparation of tricyclic spiroketones as perfumes. Patent EP 382934-A2. 1990. [Abstract: CA 114:207551].

[4] Papa AJ, Sherman PDJr. Ketones., Vol. 133rd ed New York: John Wiley and Sons; 1981.

[5] Basavaiah D, Gowriswari VVL, Bharathi TK. DABCO-catalyzed dimerization of α, ß-unsaturated ketones and nitriles. Tetrahedron Lett 1987;28:4591–4592.

[6] Ferroni R, Milani L, Simoni D, Orlandini P, Guarneri M, Franze D, Bardi A. 4-(1H-pyrazol-1-yl)-2-butylamine derivatives as inhibitors of blood platelet aggregation. Farmaco 1989; 44:495–502.

[7] Matsuda I. Michael-type addition of O-ethyl-C-O-bis(trimethylsilyl)ketene acetal and its application to the synthesis of α-xylidene-γ-lactones. J Organomet Chem 1987;321: 307–316.

[8] Nakayama M, Tanimore S, Hashio M, Mitani Y. Stereoselective synthesis of C/D/E/rings in steroids containing E (lactone) ring. Synthesis of (+)-1-(1′-hydroxyethyl)-7,7a-dihydro-5(6H)-indanone-7a-carboxylic acid-7a,1′-lactone. Chem Lett 1985;5:613–614.

[9] Kusama M, Sakuma H, Sugawara S. Low boiling compounds in cellulose cigarette smoke. Agric Biol Chem 1978;42: 479–481.

[10] Curvall M, Enzell CR, Jansson T, Pettersson B, Thelestam M. Evaluation of the biological activity of cigarette-smoke condensate fractions using six *in vitro* short-term tests. J Toxicol Environ Health 1984;14:163–180.

[11] Florin I, Rutberg L, Curvall M, Enzell CR. Screening of tobacco smoke constituents for mutagenicity using the Ames test. Toxicology 1980;15:219–232.

[12] Jonsson A, Berg S. Determination of low molecular weight oxygenated hydrocarbons in ambient air by cryogradient sampling and two-dimensional gas chromatography. Chromatography 1983;279:307–322.

[13] Westerholm R, Almen J, Hang L, Runnug U, Rosen A. Chemical analysis and biological testing of exhaust emissions from two catalyst equipped light duty vehicles operated at constant cruising speeds 70 and 90 km/h, and during acceleration conditions from idling up to 70 and 90 km/h. Sci Total Environ 1990;93:191–198.

[14] Doyle M, Sexton KG, Jeffries H, Bridge K, Jaspers I. Effects of 1,3-butadiene, isoprene, and their photochemical degradation products on human lung cells. Environ Health Perspect 2004; 112:1488–1495.

[15] Cerqueira MA, Pio CA, Gomes PA, Matos JS, Nunes TV. Volatile organic compounds in rural atmospheres of central Portugal. Sci Total Environ 2003;313:49–60.

[16] Barshteyn N, Krause RJ, Elfarra AA. Mass spectral analyses of hemoglobin adducts formed after *in vitro* exposure of erythrocytes to hydroxymethylvinyl ketone. Chem Biol Interact 2006; (In press).

[17] Sprague CL, Elfarra AA. Mercapturic acid urinary metabolites of 3-butene-1,2-diol as *in vivo* evidence for the formation of hydroxymethylvinyl ketone in mice and rats. Chem Res Toxicol 2004;17:819–826.

[18] Powley MW, Li Y, Upton PB, Walker VE, Swenberg JA. Quantification of DNA and hemoglobin adducts of 3,4-epoxy-1,2-butanediol in rodents exposed to 3-butene-1,2-diol. Carcinogenesis 2005;26:1573–1580.

[19] Powley MW, Jayaraj K, Gold A, Ball LM, Swenberg JA. 1,N2-Propanodeoxyguanosine adducts of the 1,3-butadiene metabolite, hydroxymethylvinyl ketone. Chem Res Toxicol 2003; 16:1448–1454.

[20] Krause RJ, Kemper RA, Elfarra AA. Hydroxymethylvinyl ketone: A reactive Michael acceptor formed by the oxidation of 3-butene-1,2-diol by cDNA-expressed human cytochrome P450s and mouse, rat, and human liver microsomes. Chem Res Toxicol 2001;14:1590–1595.

[21] Liu W, Zhang J, Kwon J, Weisel C, Turpin B, Zhang L, Korn L, Morandi M, Stock T, Colome S. Concentrations and source characteristics of airborne carbonyl compounds measured outside urban residences. J Air Waste Manag Assoc 2006;56: 1196–1204.

[22] Tsai SW, Hee SS. A new passive sampler for regulated workplace aldehydes. Appl Occup Environ Hyg 1999;14: 255–262.

[23] Calingasan NY, Uchida K, Gibson GE. Protein-bound acrolein: A novel marker of oxidative stress in Alzheimer's disease. J Neurochem 1999;72:751–756.
[24] Lovell MA, Xie C, Markesbery WR. Acrolein is increased in Alzheimer's disease brain and is toxic to primary hippocampal cultures. Neurobiol Aging 2001;22:187–194.
[25] Kawaguchi-Niida M, Shibata N, Morikawa S, Uchida K, Yamamoto T, Sawada T, Kobayashi M. Crotonaldehyde accumulates in glial cells of Alzheimer's disease brain. Acta Neuropathol (Berl) 2006;111:422–429.
[26] Uchida K, Kanematsu M, Morimitsu Y, Osawa T, Noguchi N, Niki E. Acrolein is a product of lipid peroxidation reaction. Formation of free acrolein and its conjugate with lysine residues in oxidized low density lipoproteins. J Biol Chem 1998;273(26):16058–16066.
[27] Lash LH, Tokarz JJ, Pegouske DM. Susceptibility of primary cultures of proximal tubular and distal tubular cells from rat kidney to chemically induced toxicity. Toxicology 1995;103: 85–103.
[28] Lash LH, Woods EB. Cytotoxicity of alkylating agents in isolated rat kidney proximal tubular and distal tubular cells. Arch Biochem Biophys 1991;286:46–56.
[29] Lash LH, Elfarra AA, Rakiewicz-Nemeth D, Anders MW. Bioactivation mechanism of cytotoxic homocysteine S-conjugates. Arch Biochem Biophys 1990;276:322–330.
[30] Kaminskas LM, Pyke SM, Burcham PC. Differences in lysine adduction by acrolein and methyl vinyl ketone: Implications for cytotoxicity in cultured hepatocytes. Chem Res Toxicol 2005;18:1627–1633.
[31] Zollner H. Inhibition of some mitochondrial functions by acrolein and methylvinylketone. Biochem Pharmacol 1973; 22:1171–1178.
[32] Mellon PL, Windle JJ, Goldsmith PC, Padula CA, Roberts JL, Weiner RI. Immortalization of hypothalamic GnRH neurons by genetically targeted tumorigenesis. Neuron 1990;5:1–10.
[33] Loikkanen J, Chvalova K, Naarala J, Vahakangas KH, Savolainen KM. Pb2 + -induced toxicity is associated with p53-independent apoptosis and enhanced by glutamate in GT1-7 neurons. Toxicol Lett 2003;144:235–246.
[34] Loikkanen JJ, Naarala J, Savolainen KM. Modification of glutamate-induced oxidative stress by lead: The role of extracellular calcium. Free Radic Biol Med 1998;24:377–384.
[35] Sathishkumar K, Murthy SN, Uppu RM. Cytotoxic effects of oxysterols produced during ozonolysis of cholesterol in murine GT1-7 hypothalamic neurons. Free Radic Res 2007;41: 82–88.
[36] Sathishkumar K, Haque M, Perumal TE, Francis J, Uppu RM. A major ozonation product of cholesterol, 3beta-hydroxy-5-oxo-5,6-secocholestan-6-al, induces apoptosis in H9c2 cardiomyoblasts. FEBS Lett 2005;579:6444–6450.
[37] Rao UM. A micellar model for investigating the chemical nature of hydrogen transfer in NAD(P)H-dependent enzymatic reactions. Biochem Biophys Res Commun 1989;159:1330–1336.
[38] Dunigan DD, Waters SB, Owen TC. Aqueous soluble tetrazolium/formazan MTS as an indicator of NADH- and NADPH-dependent dehydrogenase activity. Biotechniques 1995;19:640–649.
[39] Agrawal S, Agarwal ML, Chatterjee-Kishore M, Stark GR, Chisolm GM. Stat1-dependent, p53-independent expression of p21(waf1) modulates oxysterol-induced apoptosis. Mol Cell Biol 2002;22:1981–1992.
[40] Yadavilli S, Muganda PM. Diepoxybutane induces caspase and p53-mediated apoptosis in human lymphoblasts. Toxicol Appl Pharmacol 2004;195:154–165.
[41] Esterbauer H, Zollner H, Scholz N. Reaction of glutathione with conjugated carbonyls. Z Naturforsch [C] 1975;30: 466–473.
[42] Tjalkens RB, Luckey SW, Kroll DJ, Petersen DR. Alpha,beta-unsaturated aldehydes increase glutathione S-transferase mRNA and protein: Correlation with activation of the antioxidant response element. Arch Biochem Biophys 1998;359:42–50.
[43] Mitchell DY, Petersen DR. Inhibition of rat liver aldehyde dehydrogenases by acrolein. Drug Metab Dispos 1988;16: 37–42.
[44] Macho A, Hirsch T, Marzo I, Marchetti P, Dallaporta B, Susin SA, Zamzami N, Kroemer G. Glutathione depletion is an early and calcium elevation is a late event of thymocyte apoptosis. J Immunol 1997;158:4612–4619.
[45] Duranteau J, Chandel NS, Kulisz A, Shao Z, Schumacker PT. Intracellular signaling by reactive oxygen species during hypoxia in cardiomyocytes. J Biol Chem 1998;273: 11619–11624.
[46] Beaver JP, Waring P. A decrease in intracellular glutathione concentration precedes the onset of apoptosis in murine thymocytes. Eur J Cell Biol 1995;68:47–54.
[47] Nardini M, Finkelstein EI, Reddy S, Valacchi G, Traber M, Cross CE, van der Vliet A. Acrolein-induced cytotoxicity in cultured human bronchial epithelial cells. Modulation by alpha-tocopherol and ascorbic acid. Toxicology 2002;170: 173–185.
[48] Picklo MJ, Montine TJ, Amarnath V, Neely MD. Carbonyl toxicology and Alzheimer's disease. Toxicol Appl Pharmacol 2002;184:187–197.
[49] Kontush K, Schekatolina S. Vitamin E in neurodegenerative disorders: Alzheimer's disease. Ann N Y Acad Sci 2004; 1031:249–262.
[50] Huber A, Stuchbury G, Burkle A, Burnell J, Munch G. Neuroprotective therapies for Alzheimer's disease. Curr Pharm Des 2006;12:705–717.
[51] Boothby LA, Doering PL. Vitamin C and vitamin E for Alzheimer's disease. Ann Pharmacother 2005;39:2073–2080.
[52] Masaki KH, Losonczy KG, Izmirlian G, Foley DJ, Ross GW, Petrovitch H, Havlik R, White LR. Association of vitamin E and C supplement use with cognitive function and dementia in elderly men. Neurology 2000;54:1265–1272.
[53] Riviere S, Birlouez-Aragon I, Nourhashemi F, Vellas B. Low plasma vitamin C in Alzheimer patients despite an adequate diet. Int J Geriatr Psychiatry 1998;13:749–754.
[54] Kontush A, Mann U, Arlt S, Ujeyl A, Luhrs C, Muller-Thomsen T, Beisiegel U. Influence of vitamin E and C supplementation on lipoprotein oxidation in patients with Alzheimer's disease. Free Radic Biol Med 2001;31:345–354.